Received: 16 October 2022 | Revised: 7 February 2023 | Accepted: 12 February 2023

DOI: 10.1111/clr.14054

ORIGINAL ARTICLE

CLINICAL ORAL IMPLANTS RESEARCH WILEY

Biofilm formation on dental implants with a hybrid surface microtopography: An in vitro study in a validated multispecies dynamic biofilm model

Enrique Bravo[1] | Benjamín Serrano[2] | Honorato Ribeiro-Vidal[2,3,4] | Leire Virto[1,4] | Ignacio Sanz Sánchez[1,2] | David Herrera[1,2] | Mariano Sanz[1,2]

[1]ETEP (Etiology and Therapy of Periodontal and Peri-implant diseases) Research Group, Faculty of Odontology, University Complutense, Madrid, Spain

[2]Post-Graduate Periodontology - Faculty of Odontology, University Complutense, Madrid, Spain

[3]Department of Periodontology, Faculty of Dental Medicine, University of Oporto, Oporto, Portugal

[4]Department of Anatomy and Embryology, Faculty of Optics, University Complutense, Madrid, Spain

Correspondence
Ignacio Sanz Sánchez, Etiology and Therapy of Periodontal and Peri-Implant Diseases (ETEP) Research Group, Department of Dental Clinical Specialties, Faculty of Odontology, University Complutense of Madrid, Plaza Ramón y Cajal, s/n (Ciudad Universitaria), 28040 Madrid, Spain.
Email: ignaciosanz@ucm.es

Funding information
Mozograu

Abstract

Objectives: The objective of this study is to qualitatively and quantitatively evaluate biofilm formation on hybrid titanium implants (HS), with moderately rough and turned surface topographies.

Materials and Methods: A validated dynamic in vitro multispecies biofilm model, based on bacterial growth under flow and shear conditions resembling the oral cavity, was used to evaluate biofilm formation on the tested implant surfaces. Scanning electron microscopy (SEM) and confocal laser scanning microscopy (CLSM) were used to compare the biofilm structure and microbial biomass deposited on either the moderately rough or the turned surface of HS. Quantitative polymerase chain reaction (qPCR) was used to evaluate the total bacterial counts and counts of each specific bacterium in biofilms formed on implants with either the moderately rough or the turned surfaces, as in the hybrid titanium implants, after 24, 48 and 72 h. A general linear model was applied to compare the CLSM and qPCR results between the tested implant surfaces.

Results: A significantly higher bacterial biomass grew on the moderately rough implant surfaces, compared to the turned surface area of HS implants ($p < .05$), at all incubation times, as evidenced with both CLSM and SEM. qPCR analysis also demonstrated an important increase in the total and specific bacterial counts in moderately rough surface implants at the three incubation times.

Conclusions: Implant surface topography (moderately rough versus turned) significantly influenced in vitro biofilm formation in terms of biofilm structure, bacterial biomass and quantity of the specific species selected for the model used.

KEYWORDS
bacterial biofilm, hybrid dental implant, implant surface, in vitro, peri-implant diseases, qPCR

1 | INTRODUCTION

Dental implants have become the standard therapy for tooth replacement in total and partial edentulism, mainly due to the high long-term survival rates (between 82% and 99%) and the significant impact in the patient's quality of life (Buser et al., 2012, 2017; Corbella et al., 2021; Francetti et al., 2019; Gotfredsen, 2012). However, despite the high survival rates, it has also become evident that dental implants are not free from complications of many types. Problems related to implant failure have been associated to many factors, such as bone quality and density, smoking habit or diabetes mellitus and frequently to the advent of peri-implant diseases (Al Ansari et al., 2022; Chrcanovic et al., 2017; Mustapha et al., 2021). At the 2017 World Workshop in Periodontology, these diseases were clearly defined as inflammatory diseases of the peri-implant tissues caused by biofilm bacteria, and precise criteria were established to diagnose peri-implant health, peri-implant mucositis and peri-implantitis (Berglundh et al., 2018). Depending on the degree of the inflammatory response triggered by the biofilm accumulation on the surfaces of the implant and/or the implant supported restorations, it may affect solely the peri-implant mucosa (peri-implant mucositis) or progress deeper destroying the implant to bone interface (peri-implantitis) (Burgers et al., 2010; Ferreira Ribeiro et al., 2016). The clinical manifestations of peri-implantitis, therefore, include bleeding on probing and/or suppuration, increased probing depth and bone loss (Berglundh et al., 2018; Schwarz et al., 2018). The diagnostic accuracy of bleeding on probing as a predictor of peri-implant diseases has been evaluated in depth, with different authors advising caution with the results obtained, since factors such as abutment surface, gingival phenotype or even probing depth can influence the appearance of bleeding on probing (Coli & Sennerby, 2019; Gothberg et al., 2018; Menini et al., 2018; Nettemu et al., 2021). Different studies have demonstrated that the implant microsurface topography influence bacterial adhesion and biofilm formation, being dependent on its roughness (Bermejo et al., 2019; Bevilacqua et al., 2018; Quirynen et al., 2007; Raes et al., 2018; Sanchez et al., 2014).

Most of currently used implants are bone level implants made of moderately rough surfaces, as this surface microtopography has a significant impact on promoting early osseointegration, and these surfaces are meant to be in full contact with bone and never exposed to the oral environment (Cochran, 1999; Polizzi et al., 2013). However, this bone to implant contact may be lost, either because of early bone remodelling or due to peri-implantitis, what will result in exposure of the most coronal part of the moderately rough implant surface to the oral environment, and hence to bacterial colonization, biofilm formation and the subsequent peri-implant tissue inflammation (Subramani et al., 2009; Teughels et al., 2006), which may potentially progress to peri-implantitis (Esposito et al., 2007; Jemt et al., 2011; Marrone et al., 2013). As a possible solution to this problem, hybrid implants have been designed with a turned titanium surface in the coronal end of the implant and a moderately rough surface in the remaining implant topography. This design of hybrid implants, however, is not new, as these implants were developed when moderately rough surfaces were introduced with the objective to improve faster osteointegration through the moderately rough surface component (Davies, 1998; Lazzara et al., 1998, 1999; Sul et al., 2009; Testori et al., 2002). Currently, the objective of using these hybrid implants is to reduce the risk of peri-implant diseases in cases where the coronal portion of the implant may be exposed to the oral environment, mainly in high-risk populations.

Observational studies have reported that this implant design results in higher survival rates and significantly lesser bone loss, when compared to the standard moderately rough implants (Gallego et al., 2018). Moreover, a recent randomized clinical trial, evaluating the short-term clinical and microbiological efficacy of hybrid implants compared to conventional implants with identical design, has shown similar outcomes and excellent results in terms of the maintenance of stable peri-implant bone levels (Serrano et al., 2022). Despite these clinical findings, the microbiological colonization pattern of hybrid implants remains unclear, and it has not yet been determined whether this differential implant surface has a significant impact on biofilm formation and bacterial colonization. It was, therefore, the aim of this experimental study to evaluate the differential biofilm formation in hybrid dental implants, comparing the coronal turned with the moderately rough surface areas in the remaining implant surfaces, using a well validated in vitro multispecies biofilm dynamic model.

2 | MATERIALS AND METHODS

2.1 | In vitro multispecies dynamic biofilm model

An in vitro multispecies dynamic biofilm model (Sanchez et al., 2021) was used to evaluate biofilm formation on implant surfaces. The model consists of a series of different components, starting with a sterile recipient from which the sterile liquid culture medium is transferred to the bioreactor containing the bacterial inoculum by means of a peristaltic pump at constant pressure. This bioreactor (Lambda Minifor© bioreactor, LAMBDA Laboratory Instruments, Baar, Switzerland) maintains the culture medium under controlled environmental conditions that mimic the oral cavity (37°C, pH 7.2 and an anaerobic atmosphere [10% H_2, 10% CO_2 and the balance N_2]) and allows for the growth of the bacterial mixture at specific time periods. By means of a peristaltic pump and under continuous flow (30 mL/h), the bacterial mixture is transferred to a specifically designed Robbins device where the dental implants are held in such a way that their surfaces are located within the channel where the bacteria flows under controlled conditions and, hence, allows for biofilm formation (Sanchez et al., 2021).

To evaluate the dynamics of biofilm formation on the implant surfaces, the incubation times were set at 24, 48 and 72 h, after which, the implants were removed from the Robbins device and assessed by the corresponding technique. For quantitative polymerase chain reaction (qPCR), implants with either turned or moderately rough surfaces were used, while for confocal laser scanning

microscopy (CLSM) and scanning electron microscopy (SEM) hybrid implants were used, because these techniques allow independent evaluation of their turned and moderately rough surface areas. For each time, the protocol was repeated three times, hence, analysing a total of nine implants ($n = 9$) for qPCR and six implants ($n = 6$) for CLSM and SEM.

2.2 | Bacterial strains and culture conditions

The following bacterial strains were used: *Streptococcus oralis* CECT 907T, *Veillonella parvula* NCTC 11810, *Actinomyces naeslundii* ATCC 19039, *Fusobacterium nucleatum* DMSZ 20482, *Aggregatibacter actinomycetemcomitans* DSMZ 8324 and *Porphyromonas gingivalis* ATCC 33277. These species were cultured in blood agar plates (Blood Agar Oxoid No 2; Oxoid, Basingstoke, UK), supplemented with 5% (v/v) sterile horse blood (Oxoid), 5.0 mg/L hemin (Sigma, St. Louis, MO, USA) and 1.0 mg/L menadione (Merck, Darmstadt, Germany) at 37°C for 24–72 h in anaerobic conditions (10% H_2, 10% CO_2 and balance N_2). Pure cultures of each bacterium were grown during 24 h in anaerobic conditions in a protein-rich medium containing modified brain heart infusion (BHI) (Becton, Dickinson and Company, Franklin Lakes, NJ, USA) supplemented with 2.5 g/L mucin (Oxoid), 1.0 g/L yeast extract (Oxoid), 0.1 g/L cysteine (Sigma), 2.0 g/L sodium bicarbonate (Merck), 5.0 mg/L hemin (Sigma), 1.0 mg/L menadione (Merck) and 0.25% (v/v) glutamic acid (Sigma). After incubation, bacterial growth was accessed by spectrophotometry ($OD_{550\,nm}$) until reaching a bacterial mixture containing 10^6 colony forming units (CFU)/mL for the six bacterial strains.

2.3 | Tested implants

The hybrid surface (HS) implants used in this study had all the same dimensions (3.75 mm diameter and 10 mm length) and macroscopic design (parallel walls and a conical apex). The coronal half of the micro-thread portion of the implant (1.5 mm) and a 0.3 mm rim at the implant shoulder had a turned surface, with a mean roughness of 0.18 ± 0.06 R_a, whereas the rest of the implant had an acid-etched moderately rough surface with a mean roughness of 1.53 ± 0.24 R_a (Ticare Inhex PerioHybrid®, Mozo Grau, Valladolid, Spain). The turned portion of the implant was manufactured in the same lathe as the moderately rough surface, but it did not receive any further surface treatment such as acid-etching. R_a values were obtained by interferometric optical profilometry (Model NT1100, WYKO-Veeco, processing software Vision 32) by evaluating five different units at a random area of the implant surface. HS implants were used for the CSLM and SEM experiments. For the quantitative bacterial analysis (qPCR), fully turned or fully moderately rough surface implants were used (Ticare Inhex, Mozo-Grau, Valladolid, Spain), as it was impossible to isolate the biofilms for subsequent DNA extraction in HS implants (Figure 1).

2.4 | Confocal laser scanning microscopy (CSLM)

For quantifying the biofilm bacterial biomass, confocal images obtained from a laser scanning confocal microscope (Leica SP9, Mannheim, Germany) at the Centre of Microscopy in the National Centre for Scientific Research (CSIC) (Moncloa Campus, University Complutense of Madrid) were used. In brief, the protocol for processing the biofilms on the implant surfaces consisted of first, gently rinsing the implant surfaces with sterile phosphate buffer saline (PBS) to remove unattached bacteria and then staining the biofilms with LIVE/DEAD® BacLightTM Bacterial Viability Kit solution (Molecular Probes B. V., Leiden, The Netherlands) at room temperature. With this technique, a fluorochrome (propidium iodide, PI) was incubated (1:1 ratio) for 9 (±1) min to obtain an optimal fluorescence signal at the corresponding wavelengths (Syto9: 515–530 nm), thus, differentiating live from dead bacteria

FIGURE 1 View of (a) the hybrid implant, (b) the implant with a moderately rough surface and (c) the implant with a smoother, turned, surface.

within the biofilm. Then, the microscope (CLSM) was set up to take a series of scans (xyz) of 1 μm thickness (8 bits, 512 × 512 pixels) and obtain image stacks that were analysed with a dedicated image software (LAS X Leica®, Mannheim, Germany). From these CLSM images, the biomass of live and dead cells was calculated in micrometres^3/micrometres^2 ($\mu m^3/\mu m^2$) using the COMSTAT software (www.comstat.dk).

2.5 | Scanning electron microscopy (SEM)

HS implants were processed for SEM using the following protocol: after rinsing the implants with 2 mL PBS for 10 s, three times, a fixative solution of 4% paraformaldehyde (Panreac Química, Barcelona, Spain) and 2.5% glutaraldehyde (Panreac Química, Barcelona, Spain) was used for 4 h at 4°C. Subsequently, the samples were rinsed with PBS and sterile water (10 s in both cases) and dehydrated using a series of graded ethanol solutions (30, 50, 70, 80, 90 and 100%, with an immersion time of 10 min in each case). Finally, the implants were dried at critical point and coated with gold. Processed samples were observed at the National Centre of Electron Microscopy ICTS (University Complutense of Madrid, Madrid, Spain) with a JSM 6400 SEM, equipped with a backscattered electron detector at an image resolution of 25 kV (JSM6400, JEOL, Tokyo, Japan).

2.6 | Quantitative polymerase chain reaction (qPCR)

The implants retrieved from the Robbins device were rinsed with 2 mL PBS for 10 s, three times, sequentially, to eliminate non-adherent biofilm, placed in vials containing 1 mL PBS and vortexed for 2 min at room temperature. Once the biofilms were dispersed and further centrifuged at 13,000 rpm for 5 min, DNA from the resulting cells was extracted using a commercial kit (MolYsisComplete5; Molzym GmbH & CoKG, Bremen, Germany), following the manufacturer's instructions. With the DNA isolated from the biofilm samples, qPCR was used for detecting and quantifying the specific bacterial species used in the biofilm model. Specific primers and probes were directed against the 16S rRNA gene of each of the bacteria at optimal concentrations (*S. oralis*: 900, 900 and 300 nM; *A. naeslundii* and *P. gingivalis*: 300, 300 and 300 nM; *V. parvula*: 750, 750 and 400 nM; *A. actinomycetemcomitans*: 300, 300 and 200 nM and *F. nucleatum*: 600, 600 and 300 nM) [Life Technologies Invitrogen and Applied Biosystems (Carlsbad, CA, USA), and Roche (Roche Diagnostic GmbH, Mannheim, Germany)] (Sanchez et al., 2014). The amplification was performed in a total reaction volume of 10 μL containing 5 μL of 2 times the master mix (LC 480 Probes Master, Roche). As negative control, 2.5 μL of sterile water (NTC) was used (Roche). After an initial amplification cycle at 95°C for 10 min, 40 cycles at 95°C for 15 s and at 60°C for 1 min were carried out. The process was done using a thermal cycler (LightCycler® 480 II Roche Diagnostic GmbH, Mannheim, Germany). As plates, white FramStar 480 natural frame wells were used (4titude; The North Barn, Damphurst Lane, UK), sealed by QPCR Adhesive Clear Seals (4titude).

Each DNA sample was analysed in duplicate. The quantification cycle (Cq) values were determined on standard curves using a dedicated software (LC 480 Software 1.5, Roche Diagnosis GmbH, Mannheim, Germany). The translation between Cq values and CFU/mL was automatically generated by the software.

2.7 | Statistical analysis

For the analysis, the independent variable was the surface analysed, either turned or moderately rough. The primary outcome variable was the counts of viable bacteria present in the biofilm of each implant, measured by qPCR (on fully turned or fully moderately rough surface implants), for each tested bacterial species: *S. oralis*, *A. naeslundii*, *V. parvula*, *A. actinomycetemcomitans*, *P. gingivalis* and *F. nucleatum*. This quantitative data were expressed in CFU per mL (qPCR). As secondary outcome variables, from CLSM analysis, bacterial biomass was expressed as live/dead cell ratios obtained from the CLSM and reported as means and standard deviations (SDs). Shapiro–Wilk goodness-of-fit tests were used to assess the normality of the data distribution. Then, the ANOVA test with the Bonferroni correction to counteract the multiple comparisons was used for evaluating the differences between the two tested surfaces. Statistically significant differences were considered for p-values $<.05$. A software package (IBM SPSS Statistics 27.0, IBM Corporation, Armonk, NY, USA) was used for all data analysis.

3 | RESULTS

3.1 | SEM analysis

Scanning electron microscopy images, depicting biofilm formation on HS implants, were obtained at 24, 48 and 72 h (Figure 2). Differences in the biofilms were observed in the two defined areas (moderately rough versus turned) being the biofilms formed on turned surface areas thinner and simpler. As the maturation time progressed (from 24 to 72 h), the density of the biofilm increased, but the differences in complexity and biomass between the two surfaces areas remained.

At the highest magnification, biofilms on the turned surfaces were observed as thin, scattered along the surface, but without fully covering it, whereas biofilms formed on the moderately rough surfaces covered the full surface.

3.2 | CLSM analysis

Confocal laser scanning microscopy images depicting the biofilm formation on HS implants were obtained at 24, 48 and 72 h (Figure 3). After 24 h of incubation, the resulting biofilm biomass on

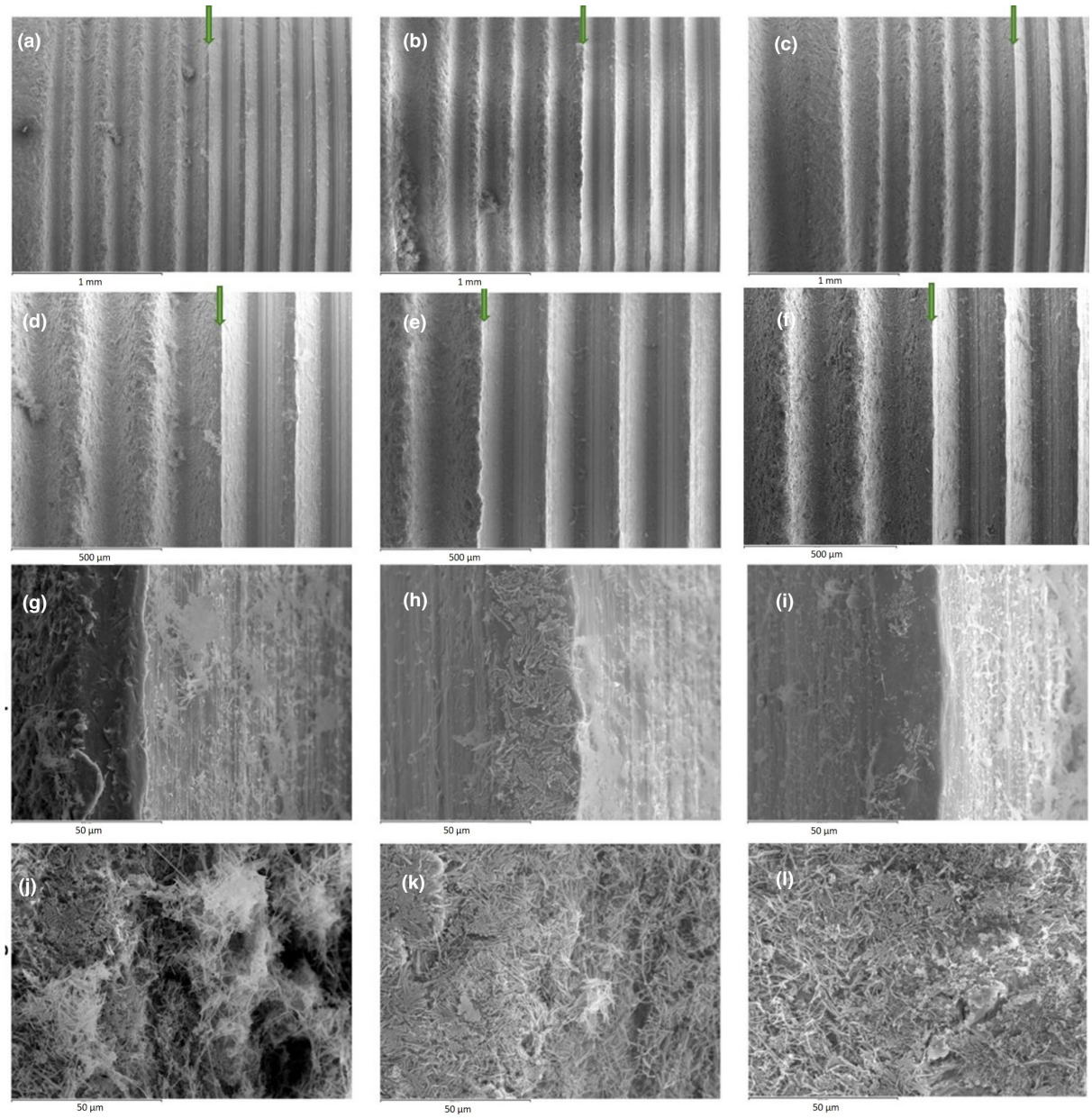

FIGURE 2 Images obtained by scanning electron microscope (SEM) of biofilms developed after 24, 48 and 72 h over hybrid implants. Images (a–c) (50×) and (d–f) (100×) showed biofilms after 24, 48 and 72 h, respectively. Images (g–i) (1000×) showed biofilms developed at 24, 48 and 72 h, respectively, over smooth surfaces; and images (j–l) showed biofilms developed at 24, 48 and 72 h, respectively, over rough surfaces of the hybrid implant. Green arrows delineate the borderline between the moderately rough surface (to the left of the arrow) and the turned surface (to the right of the arrow).

the turned and the moderately rough surface areas were 5.74 $\mu m^3/\mu m^2$ (SD = 3.53) and 11.21 $\mu m^3/\mu m^2$ (SD = 6.38), respectively. The live/dead cell ratio demonstrated higher proportion of live cells in both surfaces being 2.85 (SD = 1.81) and 3.53 (SD = 3.17) on turned and moderately rough surfaces, respectively (Figure 3a,b).

After 48 h of incubation, the total biofilm biomass was similar to that observed at 24 h, being 5.72 $\mu m^3/\mu m^2$ (SD = 2.41) on the turned surfaces (Figure 3c) and 12.91 $\mu m^3/\mu m^2$ (SD = 3.76) on the moderately rough surfaces (Figure 3d). At this time, cell vitality decreased with a live/dead cell ratio of 1.80 (SD = 1.19) and 1.57 (SD = 1.33) for turned and moderately rough surfaces, respectively.

Finally, at 72 h, biofilm biomass decreased on both surfaces (Figure 3e, smooth surface and 3f, rough surface), being 2.19 $\mu m^3/\mu m^2$ (SD = 1.86) on the turned surface and 8.98 $\mu m^3/\mu m^2$ (SD = 3.28) on the moderately rough surfaces. Similarly, there was a marked decrease in cell viability with ratios of live to dead cells of 0.60 (SD = 0.73) and 0.20 (SD = 0.10) for turned and moderately rough surfaces, respectively.

Statistically significant differences in microbial density were observed between moderately rough versus turned surfaces in all three incubation times ($p < .05$), with higher density in moderately rough surfaces. In contrast, no significant differences in cell viability were observed at any time ($p > .05$).

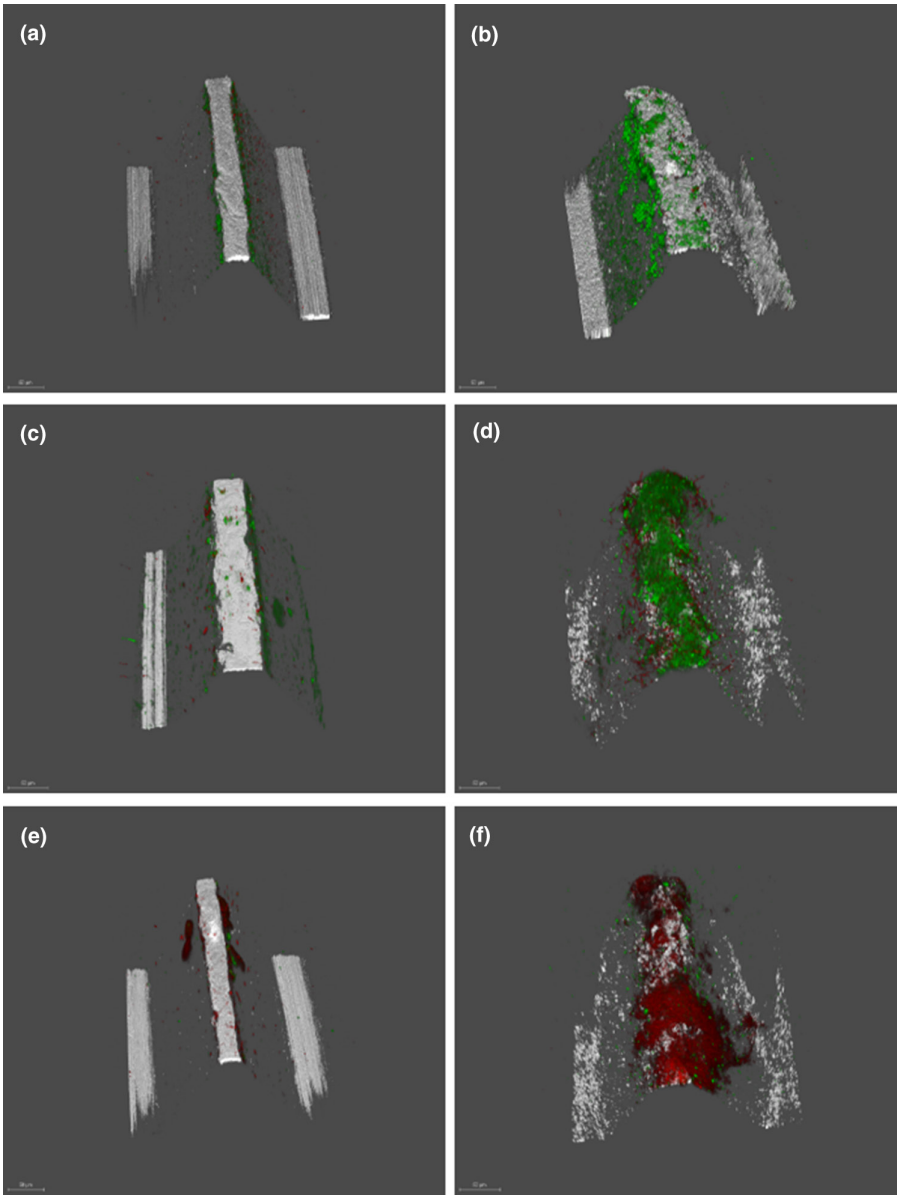

FIGURE 3 Images obtained by confocal laser scanning microscopy (CLSM) after 24 h over (a) smooth turned and (b) rough surfaces; after 48 h over (c) smooth turned and (d) rough surfaces; and after 72 h over (e) smooth turned and (f) rough surfaces of hybrid implants (scale bar = 50 μm). LIVE/DEAD® BackLight Kit was used. Live bacteria (green), dead bacteria (red) and implant surface (white) can be observed.

3.3 | Quantitative analysis by qPCR

All six bacterial species were detected by means of qPCR in both types of implants and at all incubation times. Table 1 depicts the counts of each bacterial species at both tested implants, at the three incubation times. At 24 h, higher amounts of first colonizers (*S. oralis*, *A. naeslundii* and *V. parvula*) were found in moderately rough compared with turned surface implants, being these differences statistically significant for *S. oralis* ($p = .000$). In contrast, the counts of intermediate and late colonizers (*F. nucleatum*, *P. gingivalis* and *A. actinomycetemcomitans*) were similar (Table 1). At 48 h, a similar trend was observed, with statistically significantly higher counts of *S. oralis* ($p = .003$), *A. naeslundii* ($p = .023$) and *A. actinomycetemcomitans* ($p = .030$) in the moderately rough implants, when compared with turned surface (Table 1). After 72 h, counts of *F. nucleatum* ($p = .008$), *P. gingivalis* ($p = .001$) and *V. parvula* ($p = .014$) were also significantly higher in the moderately rough surface implants (Table 1).

4 | DISCUSSION

The present study has used a validated in vitro multispecies dynamic biofilm model (Sanchez et al., 2021) to evaluate biofilm formation in HS implants, composed of a coronal turned titanium surface with the remaining surface being moderately rough. Using SEM and CLSM, statistically significant differences between surfaces were identified in the biofilm biomass and in patterns of surface colonization. Similarly, quantitative differences were

TABLE 1 Counts [expressed as mean and standard deviation (SD) and 95% confidence intervals (CI) for means, of colony-forming units (CFUs)/mL] of bacterial species, determined by quantitative polymerase chain reaction (qPCR) in 24-, 48- and 72-h biofilms formed on smooth or rough dental implants ($n = 9$), using specific primers and probes directed to the 165 rRNA gene.

			Bacterial concentration (CFU/mL)			
					95% CI	
Bacterial species	Incubation time (h)	Surface	Mean	SD	Lower limit	Upper limit
Streptococcus oralis	24	Smooth	1.54×10^7	(7.55×10^6)	9.64×10^6	2.12×10^7
		Rough	5.78×10^7	(4.21×10^7)*	2.55×10^7	9.02×10^7
	48	Smooth	1.37×10^7	(7.03×10^6)	8.27×10^6	1.91×10^7
		Rough	4.36×10^7	(2.28×10^7)*	2.61×10^7	6.11×10^7
	72	Smooth	1.02×10^7	(6.45×10^6)	5.27×10^6	1.52×10^7
		Rough	1.68×10^7	(8.45×10^6)†	1.03×10^7	2.32×10^7
Actinomyces naeslundii	24	Smooth	1.38×10^6	(1.28×10^6)	3.93×10^5	2.36×10^6
		Rough	2.56×10^6	(1.46×10^6)	1.43×10^6	3.69×10^6
	48	Smooth	1.89×10^6	(1.53×10^6)	7.16×10^5	3.07×10^6
		Rough	5.35×10^6	(4.64×10^6)*	1.78×10^6	8.91×10^6
	72	Smooth	4.53×10^6	(2.85×10^6)	2.34×10^6	6.72×10^6
		Rough	5.85×10^6	(4.77×10^6)	2.18×10^6	9.51×10^6
Veillonella parvula	24	Smooth	9.11×10^6	(6.46×10^6)	4.15×10^6	1.41×10^7
		Rough	2.88×10^7	(2.83×10^7)	7.06×10^6	5.05×10^7
	48	Smooth	2.60×10^7	(2.65×10^7)	5.65×10^6	4.64×10^7
		Rough	3.72×10^7	(3.55×10^7)	9.93×10^6	6.46×10^7
	72	Smooth	1.29×10^7	(7.36×10^6)	7.21×10^6	1.85×10^7
		Rough	4.51×10^7	(3.80×10^7)*	1.59×10^7	7.43×10^7
Fusobacterium nucleatum	24	Smooth	2.73×10^6	(2.51×10^6)	8.00×10^5	4.66×10^6
		Rough	3.73×10^6	(2.76×10^6)	1.61×10^6	5.85×10^6
	48	Smooth	2.89×10^6	(1.86×10^6)	1.46×10^6	4.32×10^6
		Rough	6.55×10^6	(4.14×10^6)	3.36×10^6	9.73×10^6
	72	Smooth	2.99×10^6	(1.77×10^6)	1.63×10^6	4.35×10^6
		Rough	8.47×10^6	(8.33×10^6)*	2.06×10^6	1.49×10^7
Porphyromonas gingivalis	24	Smooth	4.71×10^5	(3.02×10^5)	2.39×10^5	7.03×10^5
		Rough	6.26×10^5	(5.25×10^5)	2.23×10^5	1.03×10^6
	48	Smooth	7.96×10^5	(5.07×10^5)	4.06×10^5	1.19×10^6
		Rough	1.09×10^6	(7.14×10^5)	5.40×10^5	1.64×10^6
	72	Smooth	1.70×10^6	(1.04×10^6)	9.05×10^5	2.50×10^6
		Rough	3.66×10^6	(2.56×10^6)*,†	1.69×10^6	5.63×10^6
Aggregatibacter actinomycetemcomitans	24	Smooth	1.73×10^7	(1.80×10^7)	3.48×10^6	3.12×10^7
		Rough	2.52×10^7	(1.47×10^7)	1.39×10^7	3.65×10^7
	48	Smooth	2.05×10^7	(1.94×10^7)	5.56×10^6	3.54×10^7
		Rough	4.04×10^7	(3.01×10^7)*	1.73×10^7	6.36×10^7
	72	Smooth	1.43×10^7	(7.13×10^6)	8.85×10^6	1.98×10^7
		Rough	2.95×10^7	(1.64×10^7)	1.69×10^7	4.21×10^7

*$p < .05$, statistically significant differences when comparing CFU/mL over smooth and rough implants at same time interval (inter-group comparison).
†$p < .05$, statistically significant differences when comparing CFU/mL on the same implant surface (intra-group comparison) between 72 h and 24 and 48 h of grown.

found when bacterial counts were measured by means of qPCR: biofilms formed on moderately rough surface implants harboured significantly higher amounts of first colonizers in 24–48 h biofilms (*S. oralis* and *A. naeslundii*) and of intermediate and late colonizers in 48–72 h biofilms (*F. nucleatum*, *P. gingivalis* and *A. actinomycetemcomitans*) (Table 1).

These results are in agreement with previous in vitro studies demonstrating that the composition and structure of the biofilms grown on dental implants are influenced by the implant microsurface topography. However, these studies have used simpler in vitro biofilm models than the one used in the present study, either single species biofilms or multispecies biofilms but on static models (Aguayo et al., 2015; de Avila et al., 2015; Di Giulio et al., 2016; Papavasileiou et al., 2015; Pita et al., 2015; Ready et al., 2015; Sanchez et al., 2021; Schmidt et al., 2017). In fact, our research group, using the same bacterial inoculum but in the associated in vitro static biofilm model, also showed qualitative and quantitative statistically significant differences, when comparing biofilms grown on moderately rough versus turned implants surfaces (Bermejo et al., 2019). Similarly, these results also agree with those of an in vitro model with biofilm formation in layers using four periodontal-associated bacteria, grown on discs, and comparing rough versus smooth titanium surfaces, and also reporting significantly higher biofilm formation in the rough-surface discs (Violant et al., 2014). The results from the present investigation have shown, however, that cell viability ratios, although decreasing with time, were similar in both implant surfaces, in contrast with the results of a similar in vitro investigation, reporting higher cell viability on biofilms grown on rough surfaces (Bermejo et al., 2019).

This investigation has also observed that counts of the tested bacterial species, as evaluated by means of qPCR, were significantly higher in biofilms grown on moderately rough surfaces, when compared with turned surface implants, with a differential pattern of bacterial colonization, as observed in the differences among incubation times. Higher counts of first colonizers, i.e. *S. oralis* and *A. naeslundii*, were observed in moderately rough surface implants after 24 h, while intermediate and late colonizers, i.e. *F. nucleatum*, *P. gingivalis* and *A. actinomycetemcomitans*, were detected in higher numbers in moderately rough surface implants after 48 and 72 h. Differences in bacterial counts were paralleled with SEM images, depicting greater number of aggregated bacteria and spindle-shaped bacteria on the moderately rough surfaces. These results agree with other descriptive studies, based on SEM, showing that the number of adhered streptococcal chains depended on the surface topography (Pita et al., 2015). Other in vitro investigations have also reported a predominance of *Streptococcus* species (Bevilacqua et al., 2018) or *P. gingivalis* (Di Giulio et al., 2016), preferentially colonizing rough implant surfaces. However, other investigations did not find significant differences in microbial loads when comparing biofilms on different implant surfaces (Schmidt et al., 2017). In fact, one investigation reported higher counts of *V. parvula*, in smooth compared to rough surfaces (Violant et al., 2014). These differences among investigations probably reflect the heterogeneity of the different in vitro models used.

The results from the present investigation are also in agreement with data from experimental in vivo investigations, reporting higher peri-implantitis severity and increased disease progression, when experimental peri-implantitis models have been applied in implants with moderately rough compared to turned implant surfaces (Albouy et al., 2008). Similarly, human studies evaluating the efficacy of interventions to treat peri-implantitis have shown significantly worse treatment outcomes in moderately rough compared with turned titanium implants (Carcuac et al., 2017). Although the results from the present investigation cannot directly be extrapolated to a clinical scenario, the qualitative and quantitative differences observed in the biofilms may provide a reasonable explanation for the results found in the quoted clinical studies. When assessing only implant survival, a systematic review including 62 clinical studies evaluating implants with different surfaces and more than 10 years follow-up, observed high survival rates for all surfaces, and more probability of failure for turned surfaces; however, when assessing marginal bone loss, all surfaces presented poorer prognosis compared to the turned implants. The authors remarked the possible impact on the results of the differences in follow-up among studies on turned implants compared to those on modified surfaces (Wennerberg et al., 2018).

The results, however, should be interpreted with caution due to the evident limitations of the present research, such as the in vitro experimental design, or the many different variables and factors affecting the oral cavity, that cannot be reproduced in an in vitro model, which may be one of the explanations of the variability in the reported results and the heterogeneity among similar investigations (Deo & Deshmukh, 2019). Conversely, some strengths need to be highlighted, such as the use of a dynamic in vitro biofilm model, with adjusted pH, temperature and fluid dynamics, aiming to mimic the environmental conditions in the mouth. Moreover, the use of a bacterial inoculum, including first, intermediate and late colonizers, allows for studying the dynamics of bacterial colonization and biofilm formation at the different incubation times used. Furthermore, the use modified BHI culture medium on the bioreactor helps to simulate the nutrient sources available in the oral cavity (An et al., 2022; Rudney et al., 2012; Sanchez et al., 2021; Touzel et al., 2016).

Considering the listed limitations and based on the results of the present in vitro experimental study, it can be concluded that the differences in implant surface topography (moderately rough versus turned) in hybrid implants significantly influenced biofilm formation, in terms of biofilm structure, bacterial biomass and counts of specific bacterial species.

AUTHOR CONTRIBUTIONS

EB: Data collection, data interpretation, and drafting article; BS: Data interpretation and drafting article; HR-V: Concept, data collection and critical revision of article; LV: Statistics and critical revision of article; IS, DH, MS: Concept, design, approval of article and critical revision of article.

ACKNOWLEDGMENTS

We would like to thank the technical support of Dr. A.M. Vicente, at the ICTS National Centre of Electron Microscopy (University Complutense, Madrid, Spain), M.G Elvira, M.D. Hernández and M.T.

Seisdedos, at the Confocal and Fluorescence Microscopy Service of Margarita Salas Biological Research Center (Superior Center for Scientific Research) and R. Ayuso and J.E. Verdasco, at the Platform of Mechanic Workshops (University Complutense, Madrid, Spain).

CONFLICT OF INTEREST STATEMENT

The authors declare no conflict of interests with this research. This research was partially supported by a research grant from Ticare Implants (completer información).

DATA AVAILABILITY STATEMENT

The data that support the findings of this study are available from the corresponding author upon reasonable request.

ETHICAL APPROVAL

Ethics approval was not required for this in vitro study.

ORCID

Enrique Bravo https://orcid.org/0000-0002-4050-5842
Benjamín Serrano https://orcid.org/0000-0001-5021-3299
Honorato Ribeiro-Vidal https://orcid.org/0000-0002-1865-127X
Leire Virto https://orcid.org/0000-0002-3376-5232
Ignacio Sanz Sánchez https://orcid.org/0000-0002-3698-4772
David Herrera https://orcid.org/0000-0002-5554-2777
Mariano Sanz https://orcid.org/0000-0002-6293-5755

REFERENCES

Aguayo, S., Donos, N., Spratt, D., & Bozec, L. (2015). Nanoadhesion of *Staphylococcus aureus* onto titanium implant surfaces. *Journal of Dental Research*, *94*(8), 1078–1084. https://doi.org/10.1177/0022034515591485

Al Ansari, Y., Shahwan, H., & Chrcanovic, B. R. (2022). Diabetes mellitus and dental implants: A systematic review and meta-analysis. *Materials (Basel)*, *15*(9), 3227. https://doi.org/10.3390/ma15093227

Albouy, J. P., Abrahamsson, I., Persson, L. G., & Berglundh, T. (2008). Spontaneous progression of peri-implantitis at different types of implants. An experimental study in dogs. I: Clinical and radiographic observations. *Clinical Oral Implants Research*, *19*(10), 997–1002. https://doi.org/10.1111/j.1600-0501.2008.01589.x

An, S. Q., Hull, R., Metris, A., Barrett, P., Webb, J. S., & Stoodley, P. (2022). An in vitro biofilm model system to facilitate study of microbial communities of the human oral cavity. *Letters in Applied Microbiology*, *74*(3), 302–310. https://doi.org/10.1111/lam.13618

Berglundh, T., Armitage, G., Araujo, M. G., Avila-Ortiz, G., Blanco, J., Camargo, P. M., Chen, S., Cochran, D., Derks, J., Figuero, E., Hämmerle, C. H. F., Heitz-Mayfield, L. J. A., Huynh-Ba, G., Iacono, V., Koo, K. T., Lambert, F., McCauley, L., Quirynen, M., Renvert, S., … Zitzmann, N. (2018). Peri-implant diseases and conditions: Consensus report of workgroup 4 of the 2017 world workshop on the classification of periodontal and peri-implant diseases and conditions. *Journal of Periodontology*, *89*(Suppl 1), S313–S318. https://doi.org/10.1002/JPER.17-0739

Bermejo, P., Sanchez, M. C., Llama-Palacios, A., Figuero, E., Herrera, D., & Sanz, M. (2019). Topographic characterization of multispecies biofilms growing on dental implant surfaces: An in vitro model. *Clinical Oral Implants Research*, *30*(3), 229–241. https://doi.org/10.1111/clr.13409

Bevilacqua, L., Milan, A., Del Lupo, V., Maglione, M., & Dolzani, L. (2018). Biofilms developed on dental implant titanium surfaces with different roughness: Comparison between In vitro and In vivo studies. *Current Microbiology*, *75*(6), 766–772. https://doi.org/10.1007/s00284-018-1446-8

Burgers, R., Gerlach, T., Hahnel, S., Schwarz, F., Handel, G., & Gosau, M. (2010). In vivo and in vitro biofilm formation on two different titanium implant surfaces. *Clinical Oral Implants Research*, *21*(2), 156–164. https://doi.org/10.1111/j.1600-0501.2009.01815.x

Buser, D., Janner, S. F., Wittneben, J. G., Bragger, U., Ramseier, C. A., & Salvi, G. E. (2012). 10-year survival and success rates of 511 titanium implants with a sandblasted and acid-etched surface: A retrospective study in 303 partially edentulous patients. *Clinical Implant Dentistry and Related Research*, *14*(6), 839–851. https://doi.org/10.1111/j.1708-8208.2012.00456.x

Buser, D., Sennerby, L., & De Bruyn, H. (2017). Modern implant dentistry based on osseointegration: 50 years of progress, current trends and open questions. *Periodontology 2000*, *73*(1), 7–21. https://doi.org/10.1111/prd.12185

Carcuac, O., Derks, J., Abrahamsson, I., Wennstrom, J. L., Petzold, M., & Berglundh, T. (2017). Surgical treatment of peri-implantitis: 3-year results from a randomized controlled clinical trial. *Journal of Clinical Periodontology*, *44*(12), 1294–1303. https://doi.org/10.1111/jcpe.12813

Chrcanovic, B. R., Albrektsson, T., & Wennerberg, A. (2017). Bone quality and quantity and dental implant failure: A systematic review and meta-analysis. *The International Journal of Prosthodontics*, *30*(3), 219–237. https://doi.org/10.11607/ijp.5142

Cochran, D. L. (1999). A comparison of endosseous dental implant surfaces. *Journal of Periodontology*, *70*(12), 1523–1539. https://doi.org/10.1902/jop.1999.70.12.1523

Coli, P., & Sennerby, L. (2019). Is peri-implant probing causing overdiagnosis and over-treatment of dental implants? *Journal of Clinical Medicine*, *8*(8), 1123. https://doi.org/10.3390/jcm8081123

Corbella, S., Alberti, A., Calciolari, E., & Francetti, L. (2021). Medium- and long-term survival rates of implant-supported single and partial restorations at a maximum follow-up of 12 years: A retrospective study. *The International Journal of Prosthodontics*, *34*(2), 183–191. https://doi.org/10.11607/ijp.6883

Davies, J. E. (1998). Mechanisms of endosseous integration. *The International Journal of Prosthodontics*, *11*(5), 391–401.

de Avila, E. D., Lima, B. P., Sekiya, T., Torii, Y., Ogawa, T., Shi, W., & Lux, R. (2015). Effect of UV-photofunctionalization on oral bacterial attachment and biofilm formation to titanium implant material. *Biomaterials*, *67*, 84–92. https://doi.org/10.1016/j.biomaterials.2015.07.030

Deo, P. N., & Deshmukh, R. (2019). Oral microbiome: Unveiling the fundamentals. *Journal of Oral and Maxillofacial Pathology*, *23*(1), 122–128. https://doi.org/10.4103/jomfp.JOMFP_304_18

Di Giulio, M., Traini, T., Sinjari, B., Nostro, A., Caputi, S., & Cellini, L. (2016). *Porphyromonas gingivalis* biofilm formation in different titanium surfaces, an in vitro study. *Clinical Oral Implants Research*, *27*(7), 918–925. https://doi.org/10.1111/clr.12659

Esposito, M., Murray-Curtis, L., Grusovin, M. G., Coulthard, P., & Worthington, H. V. (2007). Interventions for replacing missing teeth: Different types of dental implants. *Cochrane Database of Systematic Reviews*, *4*, CD003815. https://doi.org/10.1002/14651858.CD003815.pub3

Ferreira Ribeiro, C., Cogo-Muller, K., Franco, G. C., Silva-Concilio, L. R., Sampaio Campos, M., de Mello Rode, S., & Claro Neves, A. C. (2016). Initial oral biofilm formation on titanium implants with different surface treatments: An in vivo study. *Archives of Oral Biology*, *69*, 33–39. https://doi.org/10.1016/j.archoralbio.2016.05.006

Francetti, L., Cavalli, N., Taschieri, S., & Corbella, S. (2019). Ten years follow-up retrospective study on implant survival rates and prevalence of peri-implantitis in implant-supported full-arch rehabilitations. *Clinical Oral Implants Research*, *30*(3), 252–260. https://doi.org/10.1111/clr.13411

Gallego, L., Sicilia, A., Sicilia, P., Mallo, C., Cuesta, S., & Sanz, M. (2018). A retrospective study on the crestal bone loss associated with different implant surfaces in chronic periodontitis patients under maintenance. *Clinical Oral Implants Research*, *29*(6), 557–567. https://doi.org/10.1111/clr.13153

Gotfredsen, K. (2012). A 10-year prospective study of single tooth implants placed in the anterior maxilla. *Clinical Implant Dentistry and Related Research*, *14*(1), 80–87. https://doi.org/10.1111/j.1708-8208.2009.00231.x

Gothberg, C., Grondahl, K., Omar, O., Thomsen, P., & Slotte, C. (2018). Bone and soft tissue outcomes, risk factors, and complications of implant-supported prostheses: 5-years RCT with different abutment types and loading protocols. *Clinical Implant Dentistry and Related Research*, *20*(3), 313–321. https://doi.org/10.1111/cid.12587

Jemt, T., Stenport, V., & Friberg, B. (2011). Implant treatment with fixed prostheses in the edentulous maxilla. Part 1: Implants and biologic response in two patient cohorts restored between 1986 and 1987 and 15 years later. *The International Journal of Prosthodontics*, *24*(4), 345–355.

Lazzara, R. J., Porter, S. S., Testori, T., Galante, J., & Zetterqvist, L. (1998). A prospective multicenter study evaluating loading of osseotite implants two months after placement: One-year results. *Journal of Esthetic Dentistry*, *10*(6), 280–289. https://doi.org/10.1111/j.1708-8240.1998.tb00505.x

Lazzara, R. J., Testori, T., Trisi, P., Porter, S. S., & Weinstein, R. L. (1999). A human histologic analysis of osseotite and machined surfaces using implants with 2 opposing surfaces. *The International Journal of Periodontics & Restorative Dentistry*, *19*(2), 117–129.

Marrone, A., Lasserre, J., Bercy, P., & Brecx, M. C. (2013). Prevalence and risk factors for peri-implant disease in Belgian adults. *Clinical Oral Implants Research*, *24*(8), 934–940. https://doi.org/10.1111/j.1600-0501.2012.02476.x

Menini, M., Setti, P., Pera, P., Pera, F., & Pesce, P. (2018). Peri-implant tissue health and bone resorption in patients with immediately loaded, implant-supported, full-arch prostheses. *The International Journal of Prosthodontics*, *31*(4), 327–333. https://doi.org/10.11607/ijp.5567

Mustapha, A. D., Salame, Z., & Chrcanovic, B. R. (2021). Smoking and dental implants: A systematic review and meta-analysis. *Medicina (Kaunas, Lithuania)*, *58*(1), 39. https://doi.org/10.3390/medicina58010039

Nettemu, S. K., Nettem, S., Singh, V. P., William, S. S., Gunasekaran, S. S., Krisnan, M., & Abas, A. L. (2021). Multilevel analysis of site, implant, and patient-level factors with peri-implant bleeding on probing: A cross sectional study. *International Journal of Implant Dentistry*, *7*(1), 77. https://doi.org/10.1186/s40729-021-00315-0

Papavasileiou, D., Behr, M., Gosau, M., Gerlach, T., & Buergers, R. (2015). Peri-implant biofilm formation on luting agents used for cementing implant-supported fixed restorations: A preliminary In vivo study. *The International Journal of Prosthodontics*, *28*(4), 371–373. https://doi.org/10.11607/ijp.4100

Pita, P. P., Rodrigues, J. A., Ota-Tsuzuki, C., Miato, T. F., Zenobio, E. G., Giro, G., Figueiredo, L. C., Gonçalves, C., Gehrke, S. A., Cassoni, A., & Shibli, J. A. (2015). Oral streptococci biofilm formation on different implant surface topographies. *BioMed Research International*, *2015*, 159625. https://doi.org/10.1155/2015/159625

Polizzi, G., Gualini, F., & Friberg, B. (2013). A two-center retrospective analysis of long-term clinical and radiologic data of TiUnite and turned implants placed in the same mouth. *The International Journal of Prosthodontics*, *26*(4), 350–358. https://doi.org/10.11607/ijp.3386

Quirynen, M., Abarca, M., Van Assche, N., Nevins, M., & van Steenberghe, D. (2007). Impact of supportive periodontal therapy and implant surface roughness on implant outcome in patients with a history of periodontitis. *Journal of Clinical Periodontology*, *34*(9), 805–815. https://doi.org/10.1111/j.1600-051X.2007.01106.x

Raes, M., D'Hondt, R., Teughels, W., Coucke, W., & Quirynen, M. (2018). A 5-year randomized clinical trial comparing minimally with moderately rough implants in patients with severe periodontitis. *Journal of Clinical Periodontology*, *45*(6), 711–720. https://doi.org/10.1111/jcpe.12901

Ready, D., Theodoridis, G., Green, I., Ciric, L., Pratten, J., Tay, W., & McDonald, A. (2015). In vitro evaluation of the antibiofilm properties of chlorhexidine and delmopinol on dental implant surfaces. *International Journal of Antimicrobial Agents*, *45*(6), 662–666. https://doi.org/10.1016/j.ijantimicag.2015.01.020

Rudney, J. D., Chen, R., Lenton, P., Li, J., Li, Y., Jones, R. S., Reilly, C., Fok, A. S., & Aparicio, C. (2012). A reproducible oral microcosm biofilm model for testing dental materials. *Journal of Applied Microbiology*, *113*(6), 1540–1553. https://doi.org/10.1111/j.1365-2672.2012.05439.x

Sanchez, M. C., Alonso-Espanol, A., Ribeiro-Vidal, H., Alonso, B., Herrera, D., & Sanz, M. (2021). Relevance of biofilm models in periodontal research: From static to dynamic systems. *Microorganisms*, *9*(2), 428. https://doi.org/10.3390/microorganisms9020428

Sanchez, M. C., Llama-Palacios, A., Fernandez, E., Figuero, E., Marin, M. J., Leon, R., Blanc, V., Herrera, D., & Sanz, M. (2014). An in vitro biofilm model associated to dental implants: Structural and quantitative analysis of in vitro biofilm formation on different dental implant surfaces. *Dental Materials*, *30*(10), 1161–1171. https://doi.org/10.1016/j.dental.2014.07.008

Schmidt, K. E., Auschill, T. M., Heumann, C., Frankenberger, R., Eick, S., Sculean, A., & Arweiler, N. B. (2017). Influence of different instrumentation modalities on the surface characteristics and biofilm formation on dental implant neck, in vitro. *Clinical Oral Implants Research*, *28*(4), 483–490. https://doi.org/10.1111/clr.12823

Schwarz, F., Derks, J., Monje, A., & Wang, H. L. (2018). Peri-implantitis. *Journal of Periodontology*, *89*(Suppl 1), S267–S290. https://doi.org/10.1002/JPER.16-0350

Serrano, B., Sanz-Sanchez, I., Serrano, K., Montero, E., & Sanz, M. (2022). One-year outcomes of dental implants with a hybrid surface macrodesign placed in patients with history of periodontitis: A randomized clinical trial. *Journal of Clinical Periodontology*, *49*(2), 90–100. https://doi.org/10.1111/jcpe.13575

Subramani, K., Jung, R. E., Molenberg, A., & Hammerle, C. H. (2009). Biofilm on dental implants: A review of the literature. *The International Journal of Oral & Maxillofacial Implants*, *24*(4), 616–626.

Sul, Y. T., Jonsson, J., Yoon, G. S., & Johansson, C. (2009). Resonance frequency measurements in vivo and related surface properties of magnesium-incorporated, micropatterned and magnesium-incorporated TiUnite, Osseotite, SLA and TiOblast implants. *Clinical Oral Implants Research*, *20*(10), 1146–1155. https://doi.org/10.1111/j.1600-0501.2009.01767.x

Testori, T., Del Fabbro, M., Feldman, S., Vincenzi, G., Sullivan, D., Rossi, R., Jr., Anitua, E., Bianchi, F., Francetti, L., & Weinstein, R. L. (2002). A multicenter prospective evaluation of 2-months loaded Osseotite implants placed in the posterior jaws: 3-year follow-up results. *Clinical Oral Implants Research*, *13*(2), 154–161. https://doi.org/10.1034/j.1600-0501.2002.130205.x

Teughels, W., Van Assche, N., Sliepen, I., & Quirynen, M. (2006). Effect of material characteristics and/or surface topography on biofilm development. *Clinical Oral Implants Research*, *17*(Suppl 2), 68–81. https://doi.org/10.1111/j.1600-0501.2006.01353.x

Touzel, R. E., Sutton, J. M., & Wand, M. E. (2016). Establishment of a multi-species biofilm model to evaluate chlorhexidine efficacy. *The Journal of Hospital Infection*, *92*(2), 154–160. https://doi.org/10.1016/j.jhin.2015.09.013

Violant, D., Galofre, M., Nart, J., & Teles, R. P. (2014). In vitro evaluation of a multispecies oral biofilm on different implant surfaces. *Biomedical Materials*, *9*(3), 35007. https://doi.org/10.1088/1748-6041/9/3/035007

Wennerberg, A., Albrektsson, T., & Chrcanovic, B. (2018). Long-term clinical outcome of implants with different surface modifications. *European Journal of Oral Implantology*, *11*(Suppl 1), S123–S136.

How to cite this article: Bravo, E., Serrano, B., Ribeiro-Vidal, H., Virto, L., Sánchez, I. S., Herrera, D., & Sanz, M. (2023). Biofilm formation on dental implants with a hybrid surface microtopography: An in vitro study in a validated multispecies dynamic biofilm model. *Clinical Oral Implants Research*, *34*, 475–485. https://doi.org/10.1111/clr.14054